On The Speed Stability of Wind Driven Induction Generators Connected to Distribution Systems

A. Kuperman and R. Rabinovici

Abstract—The output power and mechanical torque of a wind turbine driven induction generator, connected to a distributed system, change with the rotation speed. Furthermore, in the region corresponding to speeds above the one resulting in maximum output power, the wind turbine output power and torque decrease in a drastic manner when the rotation speed increases. Hence, the induction generator speed stabilizes even when the power system is heavily loaded and the generator terminal voltage is much lower than the nominal value. Simulation results are presented to prove the correctness of the mentioned assumptions.

Keywords—Distribution, Generation, Speed Stability, Wind Turbine

I. INTRODUCTION

DISTRIBUTED and embedded generation has recently received a lot of attention in the power industry. The penetration of induction generators (IG) in wind, hydro and thermal power plants has also rapidly increased. This fact is due to a relatively low price of induction machines, their simplicity, reliability and robustness. Hence, it is important to understand the induction generator impacts on stability related problems of distributed systems [1-3]. Freitas *et al.* [1-2] present a simulation study regarding voltage stability of distribution systems with induction generators. Behavior of power system presented in Fig. 1 is examined under different loading conditions. It has been shown, that IG terminal voltage, as well as voltage at buses 1-5 would decrease if system load increased. In addition, it has been concluded that the IG speed would increase in an unlimited and monotonic manner when the system loading factor increased above some critical value. This conclusion was based on presumption of constant mechanical torque applied to the IG, i.e. the prime

mover dynamics was neglected. However, this presumption is not valid when the prime mover is a wind turbine, whose output torque does not remain constant with the rotational speed increase.

According to [3], rotor speed stability refers to the ability of an induction (asynchronous) machine to remain connected to the electric power system and running at a mechanical speed close to the speed corresponding to the actual system frequency after being subjected to a disturbance.

This paper presents an investigation regarding small-disturbance speed stability of wind-driven induction generators under various loading conditions, taking prime mover dynamics into account. It is clearly shown, that the prime mover affects the overall system stability and performance. The prime mover stabilizing effect is demonstrated by extended simulations.

The paper is organized as follows. Sections II – IV describe the models used to represent the main system components: section II describes the model of wind turbine, used in the study; section III contains a brief description of a common gear drive train; section IV presents the mathematical description of steady-state operation of an induction generator. The methodology of analyzing the speed stability using dynamic simulations is presented in Section V. In section VI, the results are shown and discussed. The paper is concluded in Section VII.

II. THE WIND TURBINE

The power captured by a fixed-pitch wind turbine as a function of wind speed may be presented as [4-6]

$$P_t(V_\omega) = \frac{1}{2}\rho\pi R^2 C_p V_\omega^3, \tag{1}$$

where
ρ - air density (kg/m^3)
C_p - power coefficient of wind turbine
V_ω - wind velocity (m/s)
R - blade radius (m).

A wind turbine is characterized by its power coefficient (C_p) to tip-speed ratio (*TSR*) curve, where power coefficient is the ration between the energy captured by a turbine and the energy
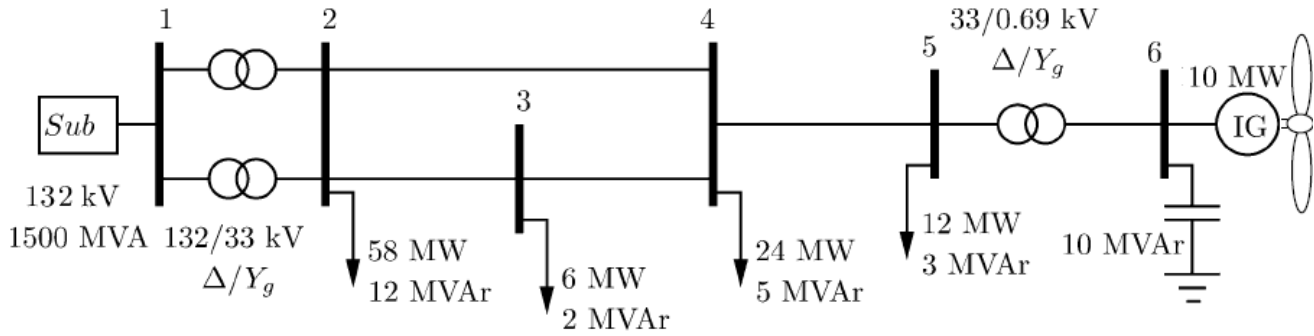
Fig. 1: Single phase diagram of the system [1]

available in the wind; the tip-speed ratio (TSR) is the ratio between the linear speed of the blade tip and the wind speed.

The *TSR* is given by

$$TSR = \frac{\omega_t R}{V_\omega} \quad , \qquad (2)$$

where

ω_t - turbine rotational speed (rad/s)
R - blade radius (m)
V_ω - wind velocity (m/s).

It is obvious from (2) that for a fixed-speed turbine the TSR is inversely proportional to the wind speed and varies across a wide range because the rotor speed of induction generator connected to a fixed-speed turbine is almost constant (depending on slip) while the wind speed varies significantly. A typical $C_p(TSR)$ curve is shown in Fig. 2. From (2), the wind speed is given by

$$V_\omega = \frac{\omega_t R}{TSR}. \qquad (3)$$
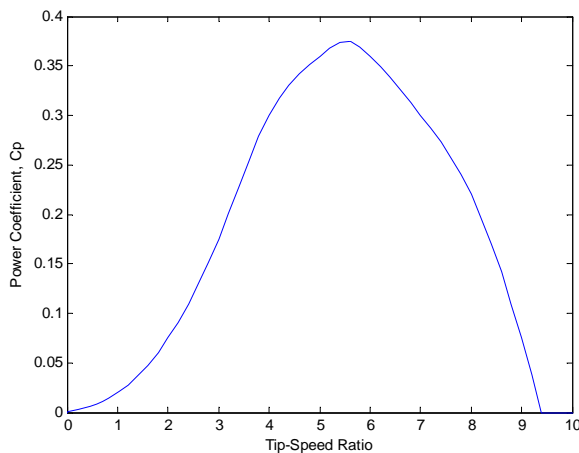
Fig. 2: Typical power coefficient C_p versus TSR

Hence, substituting (3) into (1), the power captured by a fixed-pitch wind turbine can be rewritten as a function of the turbine rotational speed:

$$P_t(\omega_t) = \frac{1}{2} \rho \pi R^2 C_p \left[\frac{R}{TSR} \right]^3 \omega_t^3 \quad . \qquad (4)$$

III. GEAR DRIVE TRAIN MECHANICS

The acceleration and deceleration of the generator rotor speed is described by the following equation [7], referred to the generator (high-speed) side:

$$(J_g^* + \frac{1}{G^2} J_t) \dot{\omega}_g + D\omega_g = \frac{1}{G} T_t^* - T_g, \qquad (5a)$$

where

J_g^* - generator inertia

J_t^* - turbine inertia

G - gear ratio (Fig. 3)

T_g - generator torque

T_t^* - turbine torque

ω_g - generator rotational speed

D - total damping constant

Eq. (5a) can be simplified to the following form:

$$J_g \dot{\omega}_g + D\omega_g = T_m - T_g, \qquad (5b)$$

where $J_g = J_g^* + \frac{1}{G^2} J_t$ is the total system inertia and

$T_m = \frac{1}{G} T_t^*$ is the turbine torque referred to the generator side.
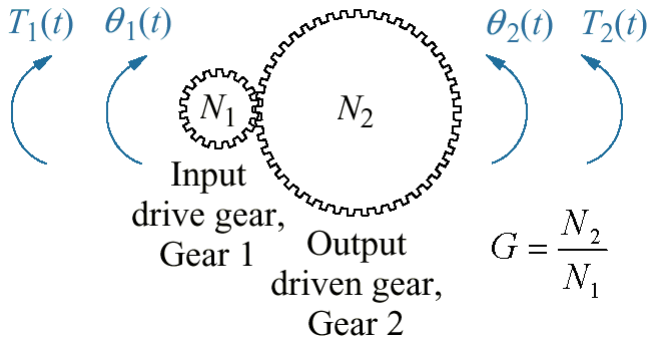
Fig.3: Typical gear (Input – generator side, Output –
turbine side)

The turbine output torque is given by

$$T_t^* = \frac{P_t - P_{t,loss}}{\omega_t} \ .$$ (6)

It is clear from (5) that when the power extracted from the
wind is higher than the power demanded by the load, the
rotor accelerates and vice-versa.

IV. INDUCTION GENERATOR

The per-unit per-phase steady state equivalent circuit of
the three-phase self-excited squirrel-cage induction
generator (IG) is shown in Fig. 3, where

R_s, R_r, R - per phase stator, rotor (referred to the stator),
and load resistances respectively

X_s, X_r, X - per phase stator, rotor (referred to the stator)
leakage, and load reactances respectively

X_m - per phase saturated magnetizing reactance

X_c - per phase terminal capacitance

F, n - per unit frequency and speed respectively
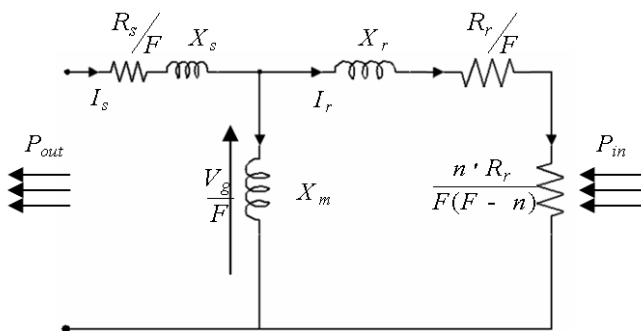
Fig. 3: Per Phase equivalent circuit of the IG

In this circuit all the generator parameters are assumed to
be constants and are independent of saturation except the

magnetizing reactance X_m. Leakage reactance and
resistance of the rotor are referred to the stator. Core loss
and effect of harmonics in the machine are neglected [8, 9].

The rotor resistance is divided into two parts; one is
representing the rotor losses, the other one (a negative
resistor) is the generated power equivalent. Both parts sum
up to one negative resistor $\dfrac{R_r}{F - n}$. The power transferred
to the generator is given by (4) assuming lossless turbine
and drive train.

According to Fig. 3, the rotor current is given by

$$I_r = \frac{V_g/F}{\dfrac{R_r}{F - n} + jX_r} \ ,$$ (7)

and its squared magnitude is given by

$$|I_r|^2 = \frac{\left(V_g/F\right)^2}{\left(\dfrac{R_r}{F - n}\right)^2 + X_r^2} \ .$$ (8)

Hence, the input and output powers are, respectively,

$$P_{in} = |I_r|^2 \frac{n \times R_r}{F(F - n)} \ ,$$ (9)

and

$$P_{out} = P_{in} - \left(|I_r|^2 \frac{R_r}{F} + |I_s|^2 \frac{R_s}{F}\right) \ .$$ (10)

The generator output torque is given by

$$T_g = \frac{P_{out}}{\omega_g} \ .$$ (11)

The generator losses vary with generator speed and should
be considered in any steady state analysis of an induction
generator. Details can be found in [10].

The induction machine, used in simulations incorporates
transient behavior as well. The overall machine operation is
hence modeled using the following equations [12], where
the electrical part of the machine is represented by a fourth-
order state-space model and the mechanical part by a
second-order system. All electrical variables and
parameters are referred to the stator. This is indicated by the
prime signs in the machine equations given below. All
stator and rotor quantities are in the arbitrary two-axis
reference frame (dq frame):

$$\frac{di_{sD}}{dt} = -\frac{1}{T_s'}i_{sD} + \frac{w_r k_r L_m}{L_s'}i_{sQ} + \frac{k_s}{T_r'}i_{rd} + \frac{w_r L_m}{L_s'}i_{rq} + \frac{u_{sD}}{L_s'}$$

$$\frac{di_{sQ}}{dt} = -\frac{w_r k_r L_m}{L_s'}i_{sD} - \frac{1}{T_s'}i_{sQ} - \frac{w_r L_m}{L_s'}i_{rd} + \frac{k_s}{T_r'}i_{rq} + \frac{u_{sQ}}{L_s'}$$

$$\frac{di_{rd}}{dt} = \frac{k_r}{T_s'}i_{sD} - \frac{w_r k_r L_s}{L_s'}i_{sQ} - \frac{1}{T_r'}i_{rd} + \frac{w_r L_r}{L_r'}i_{rq} + \frac{k_s u_{sD}}{L_r'}$$

$$\frac{di_{rq}}{dt} = \frac{w_r k_r L_s}{L_s'}i_{sD} + \frac{k_r}{T_s'}i_{sQ} + \frac{w_r L_r}{L_r'}i_{rd} - \frac{1}{T_r'}i_{rq} - \frac{k_s u_{sQ}}{L_r'}$$

$$T_g = 3L_m(i_{rq}i_{sD} - i_{rd}i_{sQ})$$

$$L_s = L_{s1} + L_m \qquad k_s = \frac{L_m}{L_s}$$

$$L_r = L_{r1} + L_m \qquad k_r = \frac{L_m}{L_r}$$

$$L_s' = \frac{L_s L_r - L_m^2}{L_r} \qquad T_s' = \frac{L_s'}{R_s}$$

$$L_r' = \frac{L_s L_r - L_m^2}{L_s} \qquad T_r' = \frac{L_r'}{R_r}$$

where

i_{sD}, i_{sD} - instantaneous values of direct- and quadrature-axis stator current components respectively and expressed in the stationary reference frame

i_{rD}, i_{rD} - instantaneous values of direct- and quadrature- axis rotor current components respectively and expressed in the stationary reference frame

L_s, L_{s1} - self- and leakage inductances of the stator respectively

L_r, L_{r1} - self- and leakage inductances of the rotor respectively

L_m - magnetizing inductance

T_s', T_r' - stator and rotor transient time constants respectively

u_{sD}, u_{sD} - instantaneous values of direct- and quadrature-axis stator voltage components respectively and expressed in the stationary reference frame

w_r - angular rotor speed

V. METHOD PRESENTATION

The methodology of analyzing the speed stability using dynamic simulations is presented in this section. The speed stability existence is derived as follows.
It is clear from (1) and (4) that wind turbine output power depends on both wind and rotation speeds. Fig. 4 presents a typical relation between wind turbine output power and rotation speed for different wind speeds [5].

Furthermore, it is clear from observing Fig. 4, that when the rotation speed increases above the value resulting in maximum output power at particular wind speed, the turbine output power reduces drastically. This is also true for turbine output torque, according to (6). Therefore the assumption of constant mechanical torque, given in [1],

should be re-examined. Since the torque, applied to the IG by wind turbine, decreases with the increase of the rotational speed on the descending part of the IG mechanical torque characteristic, the IG speed stability is achieved in this region by the above mentioned negative feedback mechanism according to (5b). Assuming no dumping without loss of generality, acceleration

($\dot{\omega}_g > 0$) is immediately followed by the turbine torque reduction ($T_m \downarrow$) and a new stable speed point is achieved.

The stability point is not feasible for the case where the stable speed is above the permitted generator/drive train/turbine mechanical speed. In such cases speed limiting usually exists [7], [10], keeping the speed constant by reducing the turbine captured power and hence, the achieved torque.
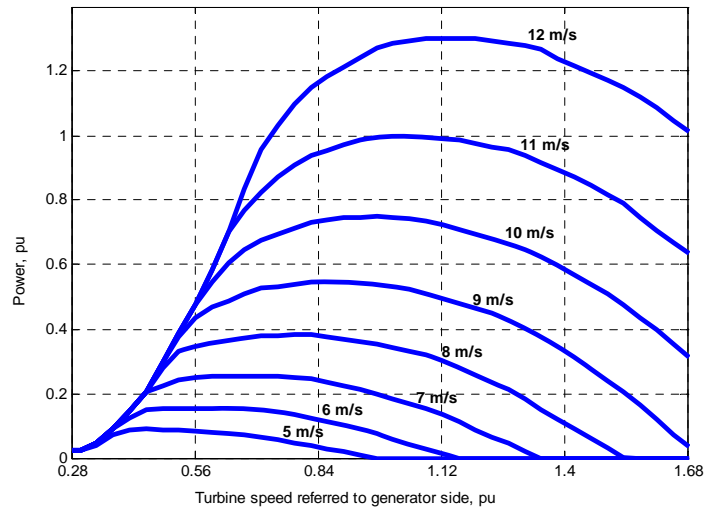
Fig. 4: Wind turbine power versus its rotation speed for different wind speeds

VI. RESULTS AND DISCUSSION

The system shown in Fig.1 was simulated with a wind turbine, whose characteristic is given in Fig. 4, taken into account. The wind speed was chosen to be 7m/s, resulting in 10MW output power at rated speed. The simulations were carried out using SimPowerSystems® Blockset of Simulink® [11].

SimPowerSystems extends Simulink® with tools for modeling and simulating basic electrical circuits and detailed electrical power systems. These tools let the user model the generation, transmission, distribution, and consumption of electrical power, as well as its conversion into mechanical power. SimPowerSystems is well suited to the development of complex, self-contained power systems, such as those in automobiles, aircraft, manufacturing plants, and power utility applications.

Simulink solvers are well suited to continuous-time (analog), discrete-time, hybrid, and mixed-signal simulations of any size. They support algebraic constraints

and state events, including discontinuities such as instantaneous changes in plant dynamics. They provide fast, reliable and accurate simulation results.

With SimPowerSystems, it is possible to use the variable-step integrators in Simulink to perform highly accurate simulations of power system models. Some of these integrators handle the numerically stiff systems that often arise in modeling real power systems. The zero-crossing detection capabilities of Simulink let the user detect and solve discontinuities with full machine precision. Together, SimPowerSystems and Simulink provide an efficient environment for multidomain modeling and controller design. By connecting the electrical parts of the simulation to other Simulink blocks, one can rapidly draw the circuit topology and simultaneously analyze the circuit's interactions with mechanical, thermal, and control systems.

SimPowerSystems provides two alternatives to continuous simulation of a power system [11]: discretization and phasor simulation, as shown in Fig. 6. Discretization simulates the system with fixed time-step trapezoidal integration, and is especially effective for power system models that include power electronic devices. This mode also facilitates the execution of the model in real time.
Phasor simulation replaces the differential equations representing the network with a set of algebraic equations at a fixed frequency. Phasor simulation facilitates transient stability studies of multi machine systems.

Phasor simulation mode was incorporated for simulating the system, since no power electronics devises were involved and the real time behavior was not important.

The baseline for the simulation was loading factor variation. Loading factor was varied from 0 to 10, giving a wide operation range from no-load to heavy load conditions. The simulations were run for 100 seconds in order to reach steady state values for all loading factors. The turbine and drive train were assumed lossless.

The simulation setup is shown in Fig. 5. The electrical network and the induction generator are modeled using SimPowerSystems blockset, while the wind turbine is modeled using Simulink.
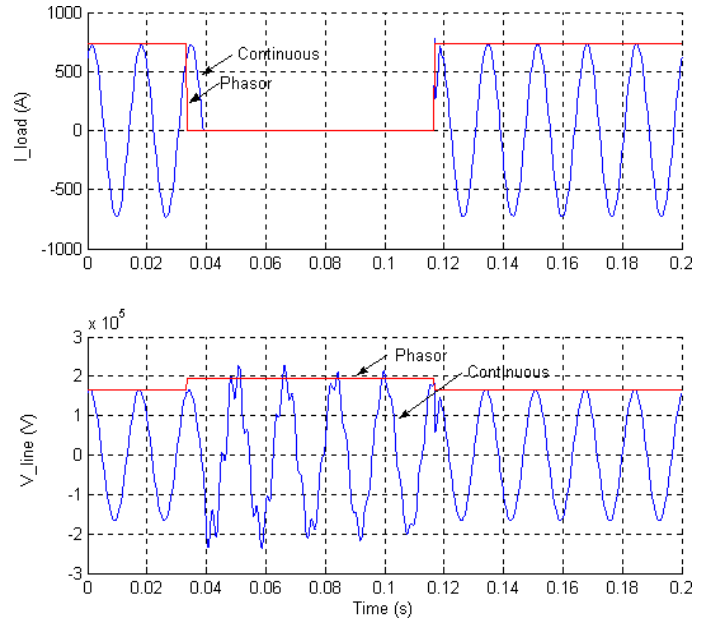
Fig. 6: Phasor vs. discretization (continuous) simulation [11]
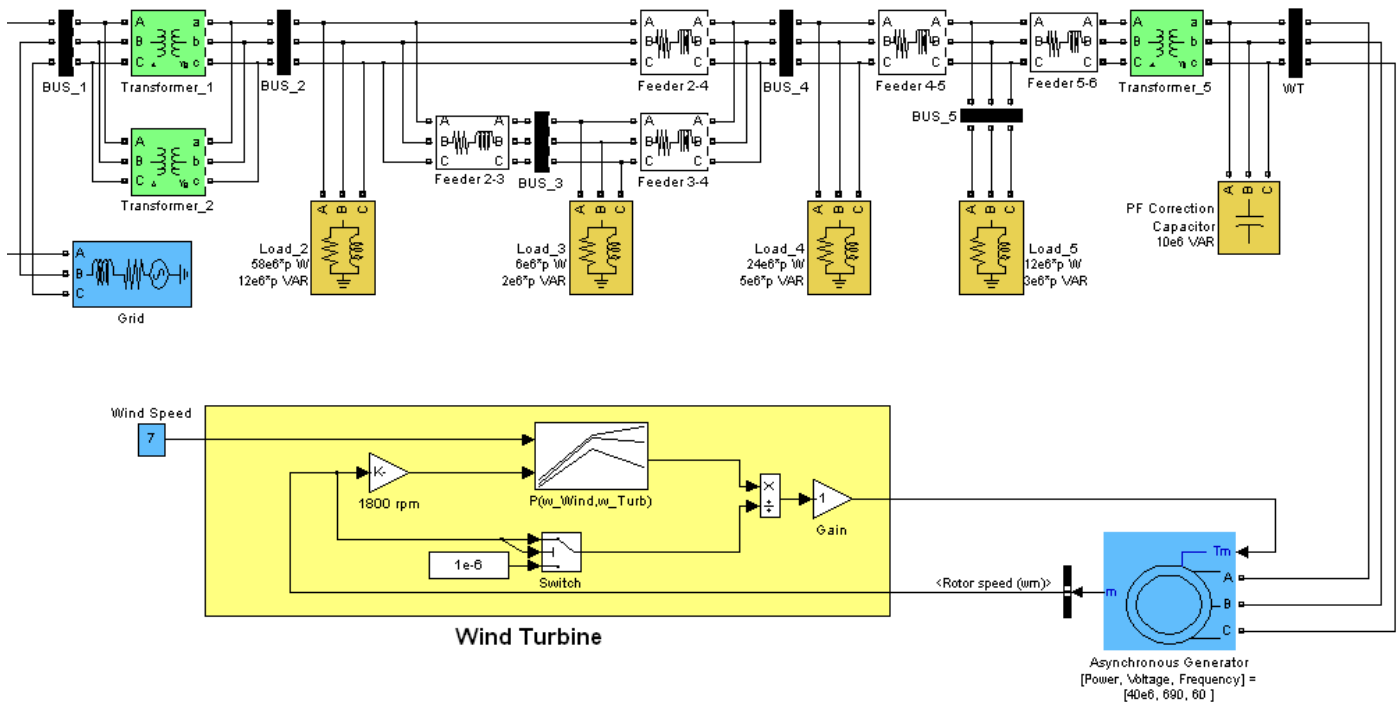
Fig.5: Combined Simulink® and SimPower® system model
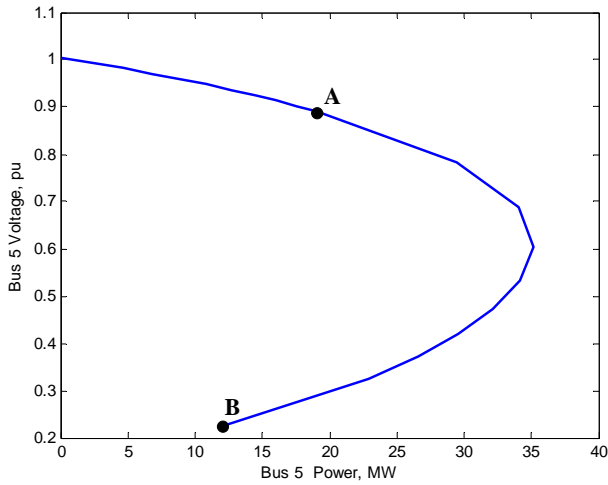
Fig. 7: PV curve of bus 5. Point A corresponds to a loading factor equal to 1, while point B corresponds to a loading factor equal to 10

First, a test simulation was performed to verify the existence of same conditions as in [1-2]. Power-voltage (PV) curve of bus 5 is shown in Fig. 7, where point A corresponds to loading factor of 1, and point B corresponds to loading factor of 10. PV Curves are the product of parametric analysis. Take into consideration the system shown in Fig 8, power is transferred from the Sending Area to the Receiving Area via a set of transmission lines forming an Interface.
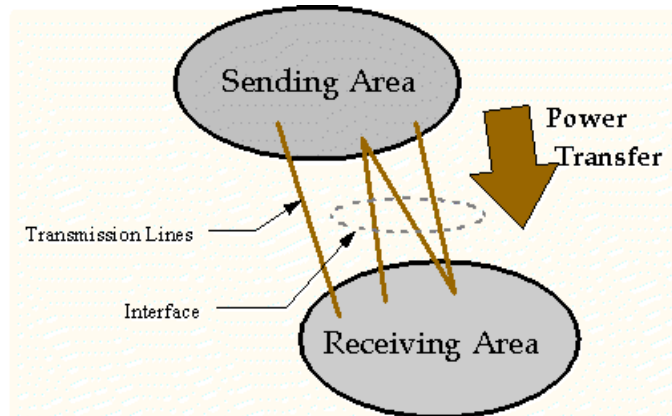
Fig. 8: PV curve concept [13]

As the transfer increases, the conditions on the lines and buses along the transfer path, including those within the Sending and Receiving area, change. The voltages may drop; current flows on branches may increase or decrease. Monitoring voltage at a particular bus and plotting this against the power transfer produces a familiar diagram known as the PV Curve. When the voltage at the selected bus goes below some pre-defined criteria, then the transfer at which this occurs is the Low Voltage transfer limit for that bus. Ignoring the low voltage and continuing to increase transfer would eventually

bring the curve to a point where the system collapses. The point of collapse can likewise be designated as the Voltage Collapse transfer limit [13].

It is clear by comparing the results with results of [1-2], that the simulated systems are similar.
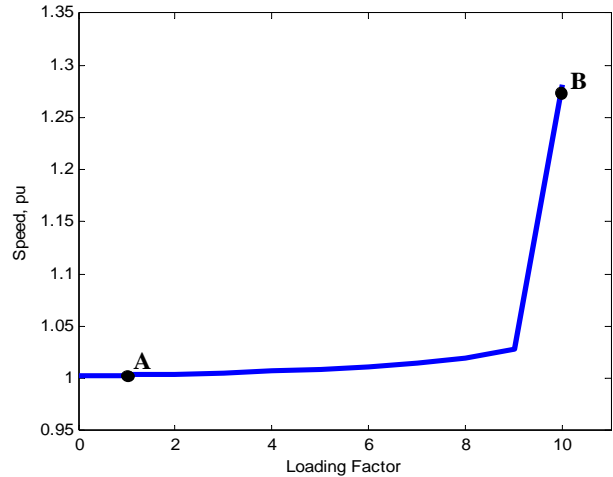
Fig. 9: Stable rotor speed versus loading factor. Point A corresponds to a loading factor of 1, while point B corresponds to a loading factor of 10.
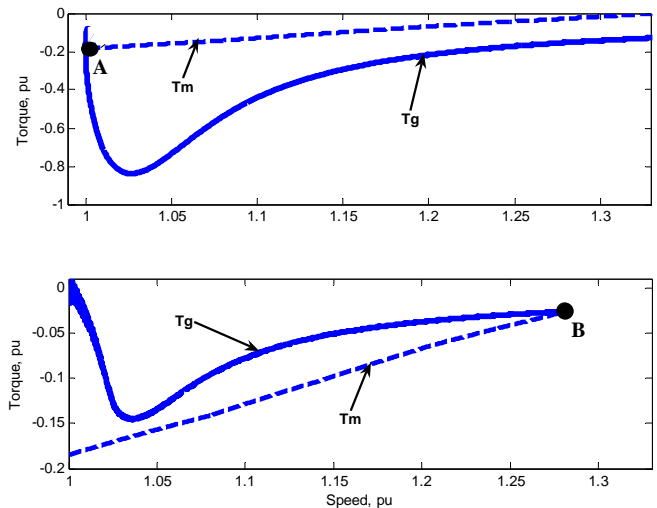
Fig. 10: Torque-speed characteristics of the IG and the wind turbine, while the wind speed is 7 m/sec and the wind turbine dynamics is also taken into account. The system loading factor is: a) 1 (point A in Figs. 5 and 6); b) 10 (point B in Figs. 5 and 6)

The IG speed reached a stable value for all the above mentioned loading factors, as shown in Fig. 9. It is clear, that with the increase of the loading factor above some value (about 9, according to Fig. 9) the rate of change in steady state value of speed increases, but a stable speed still exists for any loading factor. The results are quite easy to understand by observing Fig. 10, where electromagnetic torque of the IG and the turbine mechanical torque for loading factors of 1 and 10,

respectively, are plotted. It is obvious, that if the presumption of constant mechanical torque applied to the IG is not valid, which is true for the wind turbine output torque, but rather has a certain slope (T_m in Fig. 10), there exists a point of intersection between the torque curves. Fig. 11 presents the transient behavior of the generator speed for the above mentioned loading factors. Again, speed reaches a stable steady state value for both extreme cases.
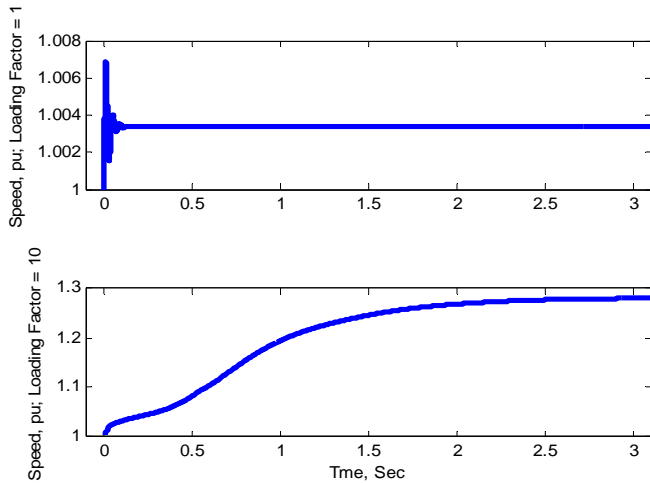
Fig. 11: Change of the IG rotation speed versus time for loading factor of a) 1, b) 10

It is clear, that for any loading factor there an equilibrium point exists, where both torqueses are equal and, hence, the speed reaches a stable value.

Speed limitation should be considered mainly because of two reasons. First, a certain level of acoustic noise should not be reached. Second, physical limitations of turbine and generator rotational speed exist and must be taken into account. If a speed limit command would have been applied, the effect was equal to the effect of additional loading of the generator and hence a stable point would be reached. However, if the stable speed point is above the turbine allowable maximum speed, as shown in Fig. 12, either the turbine must be shut down or the input power must be reduced by means of pith regulation if available.

Therefore the fact, that the turbine output torque does not remain constant with the rotational speed increase, is crucial for understanding the speed stability issue.

VII. Conclusion

When distributed systems with wind turbine driven IGs are studied, it seems that the correct assumption is that the IG prime mover output power and mechanical torque change with the rotation speed. Furthermore, in the region corresponding to speeds above the one resulting in maximum output power, the wind turbine output power and torque decrease in a rather drastic manner when the rotation speed increases. Hence, the IG speed stabilizes theoretically even when the power system is heavily loaded and the IG terminal voltage is lower than the

nominal value. Practical stability depends on the mechanical constraints of the system elements.
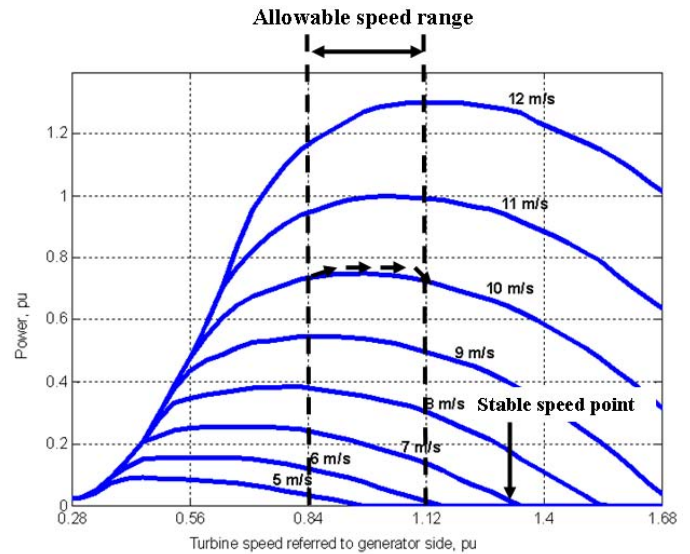
Fig. 12: Maximum allowable speed constraint

References

[1] W. Freitas, L. C. P. Da Silva, A. Morelato, "Small-Disturbance Stability of Distribution Systems With Iiduction Generators," *IEEE Trans. Power Syst.*, vol. 20, no. 3, pp. 1653-1654, 2005

[2] W. Freitas, J.C.M. Vieira, L.C.P. da Suva, C.M. Affonso and A. Morelato, "Long-term voltage stability of distribution systems with induction generators," *IEEE Power Engineering Society General Meeting*, vol.3, pp. 2910-2913, 2005

[3] O. Samuelsson, S. Lindahl, "On speed stability*," IEEE Trans. Power Syst.*, vol. 20, no. 3, pp. 1179-1180, 2005

[4] A. Kuperman, R. Rabinovici and G.Weiss, "A shunt connected inverter based variable speed wind turbine generation," *Int. Jour. of ELECTROMOTION,* vol. 13, no. 1, pp. 67-72, 2006.

[5] R. Gagnon, B. Saulnier, G. Sybille, P. Giroux; "Modeling of a Generic High-Penetration No-Storage Wind-Diesel System Using Matlab/Power System Blockset," *Global Windpower Conference*, Paris, France, April 2002.

[6] E. Muljadi, C. P. Butterfield, "Pitch-Controlled Variable Speed Turbine Generation," *IEEE Trans. Ind. Appl.*, vol 37(1), pp. 240-246, 2001

[7] N. Horiuchi, T. Kawahito, "Torque and power limitations of variable speed wind turbines using pitch control and generator power control," *IEEE Power Engineering Society Summer Meeting*, vol.1, pp. 638 - 643 2001.

[8] A. Kh. Jabri, A. I. Alolah, "Limits on the Performance of the Three-Phase Self-Excited Induction Generators", *IEEE Trans. Energy Conv.*, vol. 5(2), pp. 350-356, 1990

[9] A. Kh. Jabri, A. I. Alolah, "Capacitance requirement for Isolated Self-Excited Induction Generator", *IEE Proc.*, vol. 137(3), Pt. B, pp. 154-159, 1990

[10] A. Kuperman, R. Rabinovici and G. Weiss, "Torque and power limitations of a shunt connected inverter based WECS," *WSEAS Trans. Circuits and Systems, 7(4),* 2005

[11] *SimPowerSystems User's Guide*, TransÉnergie Technologies Inc., 2006.

[12] P. Vas, *Electrical Machines and Drives,* New York: Oxford University Press, 1992

[13] www.siemens.com

Alon Kuperman was born in Republika Moldova, in 1977. He received the B.Sc., M.Sc., Ph.D. and M.B.A. degrees from Ben-Gurion University of the Negev, Beer-Sheva, Israel, and Imperial College London in 1999, 2001, 2002 and 2006, respectively.
He was a Fellow of the Marie Curie Control Training Site with the Control and Power Group of Imperial College, London, U.K. His fields of interest are digital signal processing and control algorithms applied to the field of power electronics and electric drives.
Currently Alon is the Head of the graduate projects board at the SCE, Israel.

Raul Rabinovici (M83–SM'97) was born in Romania in 1950. He received the electrical engineering degree from the Polytechnic Institute of Jassy, Romania, in 1972 and the Ph.D. degree in electrical engineering from Ben-Gurion University of the Negev, Beer-Sheva, Israel, in 1987.
He is currently an Associate Professor with the Department of Electrical and Computer Engineering, Ben-Gurion University of the Negev. He is a Member of The Editorial Board of JEE, the Internet *Journal on Electrical Engineering*. Over the past ten years, his principal field of interest has been electric drives, including electric machines, power electronic drivers, digital signal processing operation, and control algorithms.
Prof. Rabinovici is a Member of the International Steering Committee of the Optimization of Electrical and Electronic Equipment (OPTIM) Conference, Brasov, Romania. He was a Member of the Editorial Board of The IEEE TRANSACTIONS ON MAGNETICS between 1996 and 1998.